

# Characterization of Nucleobase Analogue FRET Acceptor tC<sub>nitro</sub>

Søren Preus,<sup>†</sup> Karl Börjesson,<sup>‡</sup> Kristine Kilså,<sup>†</sup> Bo Albinsson,<sup>‡</sup> and L. Marcus Wilhelmsson<sup>\*,†</sup>

Department of Chemistry, University of Copenhagen, Universitetsparken 5, DK-2100 Copenhagen, Denmark, and Department of Chemical and Biological Engineering/Physical Chemistry, Chalmers University of Technology, S-41296 Gothenburg, Sweden

Received: October 2, 2009; Revised Manuscript Received: November 23, 2009

The fluorescent nucleobase analogues of the tricyclic cytosine (tC) family, tC and tC<sup>O</sup>, possess high fluorescence quantum yields and single fluorescence lifetimes, even after incorporation into double-stranded DNA, which make these base analogues particularly useful as fluorescence resonance energy transfer (FRET) probes. Recently, we reported the first all-nucleobase FRET pair consisting of tC<sup>O</sup> as the donor and the novel tC<sub>nitro</sub> as the acceptor. The rigid and well-defined position of this FRET pair inside the DNA double helix, and consequently excellent control of the orientation factor in the FRET efficiency, are very promising features for future studies of nucleic acid structures. Here, we provide the necessary spectroscopic and photophysical characterization of tC<sub>nitro</sub> needed in order to utilize this probe as a FRET acceptor in nucleic acids. The lowest energy absorption band from 375 to 525 nm is shown to be the result of a single in-plane polarized electronic transition oriented  $\sim 27^\circ$  from the molecular long axis. This band overlaps the emission bands of both tC and tC<sup>O</sup>, and the Förster characteristics of these donor–acceptor pairs are calculated for double-stranded DNA scenarios. In addition, the UV–vis absorption of tC<sub>nitro</sub> is monitored in a broad pH range and the neutral form is found to be totally predominant under physiological conditions with a  $pK_a$  of 11.1. The structure and electronic spectrum of tC<sub>nitro</sub> is further characterized by density functional theory calculations.

## Introduction

The development of synthetic nucleobase analogues continues to provide new tools for researchers working in the field of nucleic acids. Over the past 15 years, artificial nucleobases have been developed to enhance duplex and triplex stability,<sup>1,2</sup> to detect single nucleotide polymorphisms (SNPs),<sup>3–5</sup> as electron spin labels,<sup>6,7</sup> and to gain insight into the function of DNA polymerases,<sup>8</sup> to name but a few. In particular, fluorescent nucleobase analogues have attracted wide attention as probes for nucleic acid structure, dynamics, and interactions (for reviews, see refs 9–13). This specific class of probes includes 2-AP,<sup>14,15</sup> the pteridines 3MI and 6MI,<sup>16,17</sup> pyrrolo-C (PC),<sup>18</sup> the base discriminating fluorescent bases (BDFs) of Saito and co-workers,<sup>11,19–21</sup> the size-expanded (xDNA) nucleobases of Kool and co-workers,<sup>22,23</sup> and other more recently reported fluorescent base analogues.<sup>24–33</sup> Common for all of the mentioned fluorescent base analogues are their sensitivity to the surrounding environment and most often a significant quenching of fluorescence in the base-stacking environment provided by double-stranded DNA. These features have been exploited in applications such as quencher free molecular beacons,<sup>5</sup> in monitoring or characterizing protein activity,<sup>34–50</sup> and in probing the local structure and dynamics of nucleic acids.<sup>51–58</sup> However, the low and unpredictable fluorescence quantum yields of these fluorophores in double-stranded DNA make them highly unsuitable for studies involving fluorescence resonance energy transfer (FRET).

The two fluorescent nucleobase analogues of the tricyclic cytosine family, 1,3-diaza-2-oxophenothiazine (tC) and 1,3-

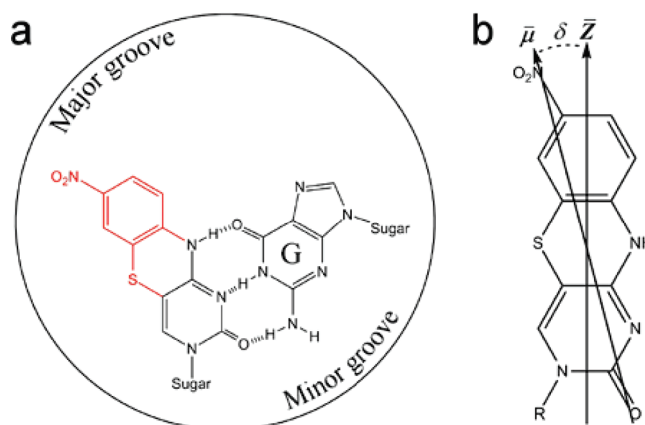


**Figure 1.** (a) Chemical structure of the tricyclic cytosine analogue tC<sub>nitro</sub> and its base-pairing with guanine. The tricyclic expansion of natural cytosine is highlighted in red. Also shown is the direction of the major and minor groove when looking down the long axis of double-stranded DNA. (b) Direction of the transition dipole moment,  $\vec{\mu}$ , associated with the lowest energy electronic transition of tC<sub>nitro</sub> ( $\delta = 27^\circ$ ). For KtC<sub>nitro</sub>, R = CH<sub>2</sub>COO<sup>−</sup>K<sup>+</sup>.

diaza-2-oxophenoxazine (tC<sup>O</sup>), have previously been characterized and shown to work excellently as fluorescent probes in both single- and double-stranded DNA.<sup>59–64</sup> The high fluorescence quantum yields and single fluorescence lifetimes, combined with a rigid and well-defined position inside the DNA double helix, make these base analogues particularly well suited for studies involving fluorescence anisotropy and FRET in nucleic acid containing systems.<sup>65</sup> Following this track, we recently demonstrated a novel FRET pair consisting of tC<sup>O</sup> as the donor and the nitro-substituted 7-nitro-1,3-diaza-2-oxophenothiazine (tC<sub>nitro</sub>, Figure 1) as the acceptor.<sup>66</sup> The well-defined position and orientation of this FRET pair inside the DNA

\* To whom correspondence should be addressed. E-mail: marcus.wilhelmsson@chalmers.se. Phone: +46 31 7723051. Fax: +46 31 7723858.

<sup>†</sup> University of Copenhagen.

<sup>‡</sup> Chalmers University of Technology.

double helix is extraordinary and facilitates an unprecedented high control of the orientation factor in the FRET efficiency compared to other labeling strategies.<sup>67–71</sup> However, in order to utilize this FRET pair for structural studies of more complex systems, the spectroscopical and photophysical properties of tC<sub>nitro</sub> must be thoroughly characterized in terms of the number of transitions constituting the lowest energy absorption band, as well as the direction and magnitude of absorbing and emitting transition dipole moments.

Here, we characterize the chromophoric properties of tC<sub>nitro</sub> with special focus put on its use as an energy acceptor in FRET experiments. In particular, we show that the lowest energy absorption band of tC<sub>nitro</sub> is the result of a single electronic transition with an in-plane polarized transition dipole moment oriented ~27° toward the NO<sub>2</sub> group from the molecular long axis (Figure 1b). In addition, the UV–vis absorption spectrum of tC<sub>nitro</sub> is monitored and shown to be preserved in a wide pH range. Furthermore, the molecular geometry of tC<sub>nitro</sub> is optimized and electronic transitions are predicted using quantum chemical calculations.

## Experimental Methods

**Synthesis.** The tC<sub>nitro</sub> nucleoside was prepared as described previously.<sup>66</sup> The potassium salt of 7-nitro-1,3-diaza-2-oxophenothiazine-3-yl acetic acid (KtC<sub>nitro</sub>) (Figure 1b) was synthesized by saponification of the tertbutyl ester, which was obtained by alkylation of the anion of 7-nitro-1,3-diaza-2-oxophenothiazine<sup>66</sup> with tertbutylbromoacetate, following the general procedure of Eldrup et al.<sup>72</sup>

**Calculations.** DFT geometry optimizations were performed in the ground state of the molecule using the B3LYP functional<sup>73–75</sup> and a 6-31G(d,p) basis set as implemented in the Gaussian 03 program package.<sup>76</sup> Restricted Hartree–Fock (RHF) wavefunctions were used. TDDFT<sup>77,78</sup> B3LYP/6-311+G(2d) calculations of the 10 lowest energy excitations were performed using Gaussian 03. The amount of HOMO → LUMO character of the lowest energy electronic transition of the investigated compound was determined from the calculated CI coefficients.

**Linear Dichroism.** Linear dichroism (LD) is the difference in absorption of two mutually perpendicular planes of linearly polarized light, and was in this work exploited to estimate the direction of the transition dipole moment of tC<sub>nitro</sub> aligned in a stretched polyvinyl alcohol (PVA) film.<sup>79</sup> The reduced LD of a uniaxial sample is defined as

$$LD^r = \frac{A_{||} - A_{\perp}}{A_{iso}} = 3 \frac{A_{||} - A_{\perp}}{A_{||} + 2A_{\perp}}$$

where  $A_{||}$  and  $A_{\perp}$  are the absorption of light oriented parallel (||) and perpendicular (⊥) to the macroscopic orientation axis (the direction of stretching) and  $A_{iso}$  is the absorbance of the corresponding isotropic sample. The LD<sup>r</sup> of a molecule with rod-like orientation is related to the angle,  $\delta_i$ , between the  $i$ th transition moment and the orientation axis by

$$LD^r = \frac{3}{2} S (\cos^2 \delta_i - 1)$$

where  $S$  is the Saupe orientation factor for the orientation axis. The LD measurements of tC<sub>nitro</sub> in stretched PVA film were performed using a Varian Cary 4B spectrophotometer equipped with Glan air-space calcite polarizers in both sample and reference beam. The film was made from a 12.5% (w/w) aqueous solution of PVA that was prepared by dissolving PVA in water under heating to 85–95 °C and continuous stirring. A

5 mL portion of the transparent PVA solution was mixed with 3 mL of an aqueous solution of the potassium salt of tC<sub>nitro</sub> (~0.2 mg of substance). The mixture was poured onto rinsed horizontal glass plates and left to dry in a dust-free environment for a week. The film was then removed from the plates and mechanically stretched 4 times the original length under hot air from a hairdryer using a manually operated, in-house built device.

**Fluorescence Anisotropy.** Fluorescence anisotropy,  $r$ , measurements were performed by exciting the sample using vertically polarized light, and it was calculated as the intensity ratio between the polarized and total emission emanating from the sample<sup>80</sup>

$$r = \frac{I_{||} - GI_{\perp}}{I_{||} + 2GI_{\perp}}$$

Here,  $I_{||}$  and  $I_{\perp}$  are the emission intensities measured through polarizers oriented parallel and perpendicular to the incident wave, respectively, and the  $G$ -factor is the ratio of the instrumental sensitivities for vertically and horizontally polarized light. For an immobile fluorophore, the angle between absorbing and emitting transition moments,  $\alpha$ , is related to the fundamental anisotropy by

$$r_0 = \frac{1}{5} (3 \cos^2 \alpha - 1)$$

The fundamental fluorescence anisotropy of tC<sub>nitro</sub> was measured by immobilizing the molecule in a propylene glycol (PG) glass at 200 K using an Oxford optistat DN cryostat and measuring the excitation spectrum through Glan polarizers in both excitation and emission beam. Spectra were recorded on a Spex Fluorolog 3 spectrofluorimeter (JY Horiba) using excitations in the range 290–510 nm in 4 nm intervals with the emission monitored at 530 nm.

**Magnetic Circular Dichroism.** In magnetic circular dichroism (MCD), two CD spectra are recorded of the sample in the presence of a magnetic field oriented from north to south and south to north. The MCD spectrum is then calculated by subtracting the two<sup>79,81</sup>

$$2MCD(\lambda) = NS(\lambda) - SN(\lambda)$$

where NS and SN represent the measured CD with the magnetic field oriented north–south and south–north, respectively. In the presence of an external magnetic field, two electronic transitions close in energy but with different polarizations will split into two MCD signals of opposite sign, resulting in a bisignate signal over the absorption band. Thus, MCD is a useful method to determine whether an absorption band contains one or several transitions. The MCD of tC<sub>nitro</sub> was measured on a Jasco-J-720 CD spectropolarimeter equipped with a permanent horseshoe magnet. The MCD signal was recorded in the range 300–550 nm at a rate of 20 nm/min, and the final spectrum was determined as an average of eight acquisitions. A baseline of the solvent, a water/methanol (1:2) mixture, was used for both the NS and SN acquisitions. The concentration of the tC<sub>nitro</sub> nucleoside was 240 μM.

**UV–vis Absorption.** UV–vis absorption spectra were recorded on a Varian Cary 4000 spectrophotometer in 1 cm quartz cuvettes using pure solvent as the baseline.

The pH titration of tC<sub>nitro</sub> was performed by mixing a set of samples from aqueous stock solutions of tC<sub>nitro</sub>, 2 M KOH, and 1 M HCl producing 10–12 samples of equal tC<sub>nitro</sub> concentrations but different pH values. The pH range was tested from pH 0.2 to 12.2 and measured on a standard calibrated pH meter.

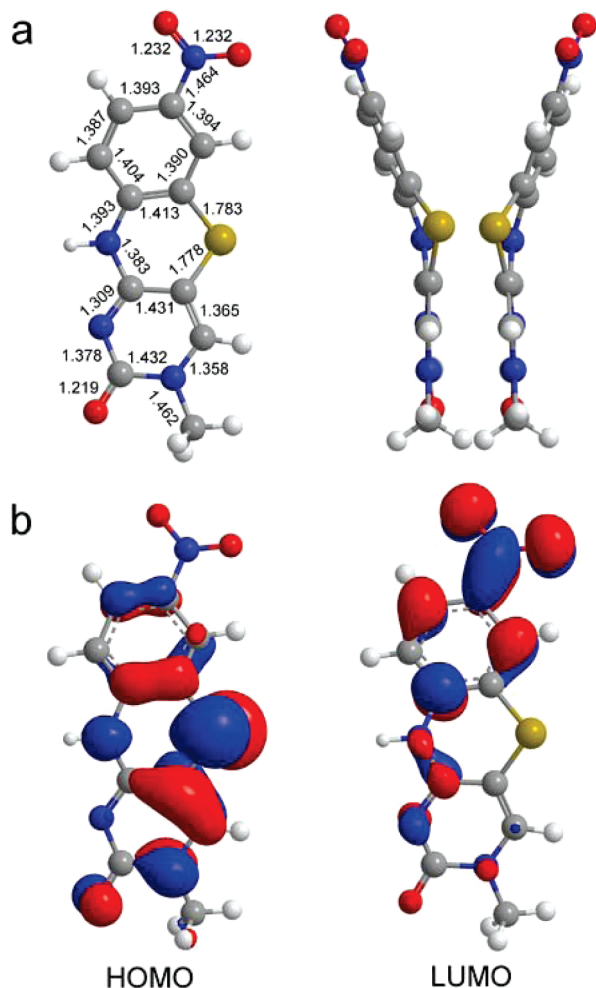


**Figure 2.** (a) B3LYP/6-31G(d,p) optimized ground state structures of the isolated  $tC_{\text{nitro}}$  base. Two local energy minima were identified on the PES of  $tC_{\text{nitro}}$  corresponding to geometries folded along the middle sulfur–nitrogen axis. Left: front view. Right: side view. Bond lengths are given in Ångströms. (b) Frontier KS orbitals of  $tC_{\text{nitro}}$  optimized at the B3LYP/6-311+G(2d) level.

Singular value decomposition (SVD) is a mathematical tool with application in the deconvolution of spectra resulting from several absorbing species.<sup>82</sup> SVD analysis was performed using an in-house built Matlab script. The pH was rewritten into a vector of  $[H^+]$  and used with a matrix containing the experimentally recorded spectra with each column representing a pH value and rows representing wavelengths. The  $pK_a$  was determined from the  $[H^+]$  at which the ratio between the protonated and deprotonated components in the SVD analysis was 1.

## Results and Discussion

**Molecular Geometry and Electron Distribution.** The strict conditions set by the DNA double helix on a nucleobase analogue in terms of H-bonding, base-stacking, and steric hindrances make it highly relevant to determine the molecular geometry of  $tC_{\text{nitro}}$ . Two local energy minima on the potential energy surface of  $tC_{\text{nitro}}$  were identified from a B3LYP/6-31G(d,p) conformational search (Figure 2a). Calculations of the vibrational spectra confirmed that the optimized structures correspond to minima on the potential energy surface. As seen in Figure 2a, the two different geometries are the result of a distortion of the tricyclic framework symmetry due to the large sulfur atom present in the middle ring. The two local minima

are mirror images corresponding to two geometries folded along the middle sulfur–nitrogen axis. This is also the result of AM1 calculations performed on the structurally similar  $tC$  base.<sup>64</sup> However, a slight distortion of the sulfur atom from the molecular plane is predicted by the DFT calculations compared to the AM1 optimized geometry. This is accompanied by a larger degree of bending (an angle of  $26^\circ$  for the DFT optimized geometry compared to  $18^\circ$  for AM1). The result that  $tC_{\text{nitro}}$  adopts a bent geometry is supported by the X-ray structure of the parent compound phenothiazine.<sup>83,84</sup>

The bent geometries of  $tC_{\text{nitro}}$  (and  $tC$ ) do not affect the B-DNA secondary structure sterically, since the expansion of these base analogues, compared to natural cytosine, is directed into the major groove of B-DNA. In addition, given the structural similarities between  $tC$ ,  $tC^O$ , and  $tC_{\text{nitro}}$ , as well as the fact that  $tC_{\text{nitro}}$  does not decrease duplex stability nor perturb the B-DNA structure in any significance,<sup>66</sup> we find it very likely that the base-flipping rate of  $tC_{\text{nitro}}$  is as slow as that of  $tC$  and  $tC^O$ .<sup>60–62</sup> Furthermore, a very pronounced relationship between the DNA double helical structure and previously measured FRET efficiencies between  $tC^O$  and  $tC_{\text{nitro}}$  positioned inside double-stranded DNA supports the claim that  $tC_{\text{nitro}}$  is firmly stacked inside the DNA double helix.<sup>66</sup>

The two optimized frontier Kohn–Sham (KS) orbitals of  $tC_{\text{nitro}}$  are shown in Figure 2b. The HOMO orbital is distributed almost throughout the entire molecular plane (although with low density at the nitro group), while the LUMO orbital is mainly centered at the electron withdrawing nitro group. As a result of the small spatial overlap of the HOMO and LUMO orbitals of  $tC_{\text{nitro}}$ , the lowest energy electronic transition has a certain degree of charge-transfer character, which is a characteristic often seen for polycyclic nitroaromatics.<sup>85–88</sup>

**Calculations of Electronic Transitions and Frontier Orbitals.** The UV–vis absorption spectrum of the nucleoside of  $tC_{\text{nitro}}$  in  $H_2O$  at 295 K is shown in Figure 3a. The lowest energy absorption band is centered at 424 nm ( $\epsilon_{424 \text{ nm}} = 5400 \text{ M}^{-1}\text{cm}^{-1}$ ) but becomes slightly red-shifted (10–15 nm) upon incorporation into DNA.<sup>66</sup> This Gaussian-shaped band is energetically well separated from higher energy absorption bands ( $\Delta E \sim 1 \text{ eV}$ ).

The TDDFT B3LYP/6-311+G(2d) calculated electronic spectrum of the B3LYP/6-31G(d,p) optimized molecular geometry of  $tC_{\text{nitro}}$  is also depicted in Figure 3a (vertical lines). In general, the overall appearance of the calculated spectrum agrees well with the experimentally recorded UV–vis absorption spectrum in  $H_2O$ . The lowest energy absorption band of  $tC_{\text{nitro}}$  is found to be the result of a single electronic transition having 92% HOMO  $\rightarrow$  LUMO character which is energetically well separated from higher energy transitions ( $\Delta E \sim 1 \text{ eV}$ ). The direction of the calculated transition dipole moment associated with the  $S_0 \rightarrow S_1$  transition was predicted to be oriented in-plane and tilted  $9^\circ$  toward the nitro group from the molecular long axis. The direction of the transition dipole moment of  $tC_{\text{nitro}}$  does not change when interconverting between the two bent geometries.

It is noted here that the CT character of most of the excited states of  $tC_{\text{nitro}}$  (data not shown for transitions above the lowest in energy) results in slightly underestimated excitation energies, which is a well-known problem when using local functionals, such as B3LYP, in the prediction of excitation energies of transitions involving KS orbitals of small spatial overlap.<sup>89–91</sup> The excitation energies shown in Figure 3a have therefore been multiplied by a factor 1.08 to facilitate comparison with the overall spectral shape of the UV–vis absorption spectrum of  $tC_{\text{nitro}}$  in  $H_2O$ .



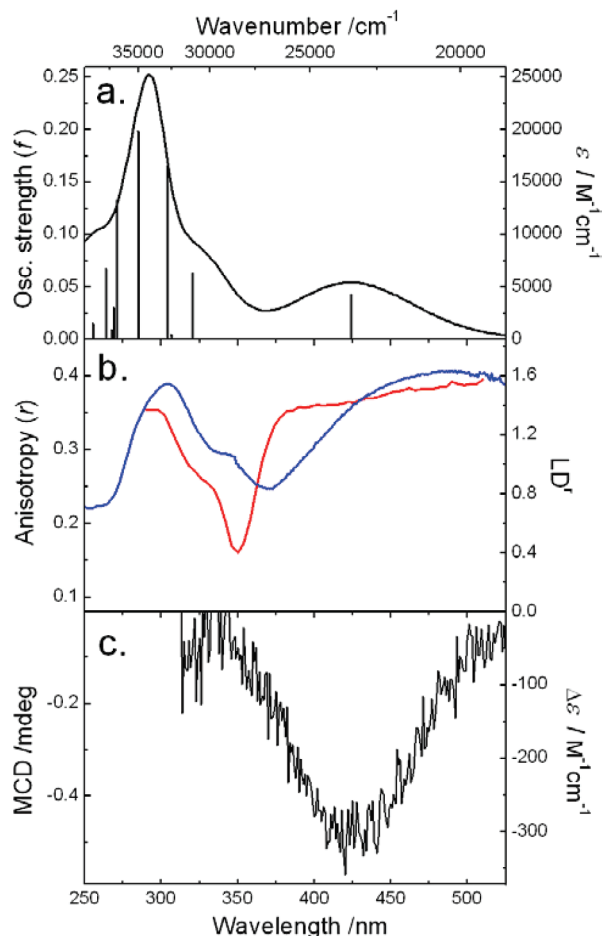


**Figure 3.** (a) Isotropic UV-vis absorption spectrum (full drawn line) and calculated electronic transitions (vertical lines). The absorption spectrum was measured in  $H_2O$  at 295 K. Electronic transitions were predicted in the gas phase at the TDDFT B3LYP/6-311+G(2d) level. Note that the calculated excitation energies have been multiplied by a factor of 1.08 to facilitate comparison with the UV-vis absorption spectrum in  $H_2O$ . (b) Excitation anisotropy spectrum (red) of the  $tC_{\text{nitro}}$  nucleoside and reduced linear dichroism spectrum (blue) of the potassium salt of  $tC_{\text{nitro}}$ . The anisotropy was measured in a propylene glycol glass at 200 K, and the linear dichroism was recorded using a stretched PVA film. (c) MCD spectrum of  $tC_{\text{nitro}}$  nucleoside in a  $H_2O$ /methanol mixture (1:2).

**Experimental Characterization of the Lowest Energy Absorption Band.** The electronic transition responsible for the lowest energy absorption band of  $tC_{\text{nitro}}$  was experimentally characterized using three different polarized optical spectroscopy techniques: fluorescence anisotropy, MCD, and LD. Figure 3b shows the fluorescence anisotropy of the nucleoside of  $tC_{\text{nitro}}$  immobilized in a PG glass at 200 K (red). The change from  $H_2O$  to PG does not change the shape of the absorption spectrum of the chromophore and only slightly shifts the absorption maximum of the lowest energy band to higher energy (5 nm; data not shown). As can be seen, the excitation anisotropy of  $tC_{\text{nitro}}$  almost reaches the theoretical maximum value of  $r_A = 0.4$  over the lowest energy absorption band. First of all, this shows that the fluorophore is practically immobilized on the time scale of the excited state decay. Second, this value of  $r_A$  corresponds to completely parallel absorbing and emitting transition dipole moments. Combined with the fact that  $r_A$  is essentially constant over the entire lowest energy absorption band, this indicates that the low energy absorption band of  $tC_{\text{nitro}}$  only contains a single electronic transition which, in turn, is the  $S_0 \rightarrow S_1$  transition.

The MCD of the nucleoside of  $tC_{\text{nitro}}$  in a  $H_2O$ /methanol mixture (1:2) is shown in Figure 3c. The use of a  $H_2O$ /methanol mixture as solvent was necessary in order to dissolve a sufficient amount of sample to detect the MCD signal. The change from pure  $H_2O$  to a  $H_2O$ /methanol mixture does not change the absorption spectrum of  $tC_{\text{nitro}}$  significantly (data not shown). As seen from Figure 3c, the MCD signal over the region of the lowest absorption band of  $tC_{\text{nitro}}$  bears the same sign and appears as the mirror image of the absorption spectrum. Together with the fluorescence anisotropy measurement and the high level quantum chemical calculations (*vide supra*), this result strongly indicates that only a single electronic transition is responsible for the lowest energy absorption band of  $tC_{\text{nitro}}$ .

The direction of the  $S_0 \rightarrow S_1$  transition dipole moment of  $tC_{\text{nitro}}$  was estimated on the basis of the reduced linear dichroism of the potassium salt of  $tC_{\text{nitro}}$  (Figure 1b where  $R = CH_2COO^-K^+$ ) aligned in a stretched polyvinyl alcohol (PVA) film (Figure 3b, blue line). As can be seen, the  $LD'$  of  $tC_{\text{nitro}}$  reaches a value of  $LD' = 1.62$  over the lowest energy absorption band. Assuming that  $tC_{\text{nitro}}$  orients similarly to the structurally comparable compound methylene blue within the PVA film (rod-like with a Saupe orientation factor of 0.78)<sup>92</sup> as previously assumed for  $tC$  and  $tC^O$  aligned in stretched PVA films,<sup>61,64</sup> the direction of the absorbing transition moment of  $tC_{\text{nitro}}$  is calculated to be tilted  $27^\circ$  from the molecular long axis. The TDDFT calculations (*vide supra*) together with a FRET study in double-stranded DNA<sup>66</sup> have shown that the tilt is toward the nitro group. The fact that the  $LD'$  is not constant over the entire absorption band of  $tC_{\text{nitro}}$  was also observed for the  $LD'$  of  $tC$  and  $tC^O$ .<sup>61,64</sup> This feature may be the result of several absorbing species oriented differently in the film, such as aggregates of molecules formed due to the high sample concentration used in the film.

**Emissive Properties.** The fluorescence quantum yield of  $tC_{\text{nitro}}$  is virtually zero, both in its monomeric form and after incorporation into single- and double-stranded DNA, but increases at temperatures below 225 K with an emission band centered at 530 nm in PG (data not shown). The weak or complete lack of fluorescence is a general property of nitroaromatic compounds and is usually either due to a fast intersystem crossing<sup>88,93–95</sup> or internal conversion<sup>85,96</sup> process. For  $tC_{\text{nitro}}$ , we suggest that the quenching is due to an efficient  $S_1 \rightarrow S_0$  internal conversion related to the charge transfer character of the first excited state. Studies addressing this are currently performed in our lab.

**pH Dependency.** The pH range of the neutral form of  $tC_{\text{nitro}}$  was investigated by monitoring the UV-vis absorption of  $tC_{\text{nitro}}$  at various pH values. The experiment shows that the neutral form of  $tC_{\text{nitro}}$  is predominant in a pH range from pH 11 down to at least pH 0.2 (the most acidic pH tested). The result of a pH 8–12 titration of the nucleoside of  $tC_{\text{nitro}}$  in  $H_2O$  is shown in Figure 4a in which the arrows denote the spectral evolution as the pH increases. When increasing the pH, the low energy absorption band of  $tC_{\text{nitro}}$  at  $\lambda_{\text{max}} = 424$  nm is replaced by a more intense band at  $\lambda_{\text{max}} = 500$  nm corresponding to the deprotonated compound (deprotonation of the central enamine). The color of the sample correspondingly changes from a clear yellow to a deep red color. The presence of several isosbestic points on the titration curves (at 227, 253, 306, 387, and 436 nm) strongly indicates that only the protonated and deprotonated forms of  $tC_{\text{nitro}}$  are present in the solution.

Since the measured absorption spectrum of  $tC_{\text{nitro}}$ , at each of the different pH values, is a linear combination of the absorption spectra of the protonated and deprotonated species, the isolated

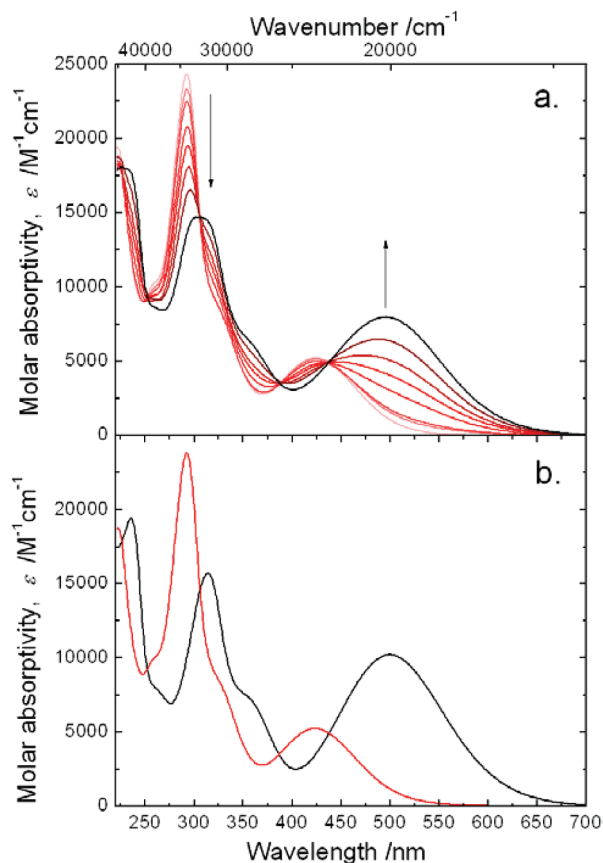


**Figure 4.** (a) Isotropic absorption spectra of  $tC_{\text{nitro}}$  at various pH values. Arrows indicate an increase in pH. pH values used: 8.00, 9.88, 10.22, 10.74, 10.89, 11.13, 11.34, 11.74, and 12.18. (b) Isolated spectra of the protonated (red) and deprotonated (black) of  $tC_{\text{nitro}}$  in  $H_2O$  obtained from the singular value decomposition (SVD).

absorption spectrum of each of the two components can successfully be deconvoluted using singular value decomposition. The isolated spectra obtained from the SVD analysis are shown in Figure 4b. The overall isolated absorption spectrum of the deprotonated component is red-shifted compared to the neutral compound. This is most likely due to electrostatic interactions with the solvent resulting from the net negative charge of the deprotonated compound. The red-shift in wavenumbers is  $3500\text{ cm}^{-1}$  for the lowest energy absorption band and  $2400\text{ cm}^{-1}$  for all of the higher energy absorption maxima and the shoulder at  $350\text{ nm}$ . This suggests that the energy of  $S_0$  of  $tC_{\text{nitro}}$  is increased by  $0.30\text{ eV}$  ( $2400\text{ cm}^{-1}$ ) for the deprotonated anion, while the  $S_1$  energy is stabilized by  $0.14\text{ eV}$  ( $3500 - 2400\text{ cm}^{-1} = 1100\text{ cm}^{-1}$ ), compared to the neutral protonated species in  $H_2O$ .

The  $pK_a$  of  $tC_{\text{nitro}}$  is calculated from the SVD analysis to be 11.1. This  $pK_a$  value of  $tC_{\text{nitro}}$  is 2 units lower than that found for  $tC$  ( $pK_a = 13.2$ ),<sup>64</sup> most likely due to the electron-withdrawing  $NO_2$  group that stabilizes the negative charge of the deprotonated compound.

**Förster Characteristics.** The red-shifted absorption of  $tC_{\text{nitro}}$  has a considerable spectral overlap with the fluorescence spectra of both  $tC$  and  $tC^O$ . In Table 1, we have summarized the calculated overlap integrals<sup>80</sup> between the nucleobase analogue FRET pairs of the tricyclic cytosine family. Because the absorption and emission spectra, as well as the fluorescence quantum yields, of the nucleobase analogues change upon incorporation into DNA, the overlap integrals are also shown for the FRET pairs positioned in double-stranded DNA.

**TABLE 1: Calculated Overlap Integrals and Critical Förster Distances (for  $\kappa^2 = 2/3$ ) of the  $tC$ – $tC_{\text{nitro}}$  and  $tC^O$ – $tC_{\text{nitro}}$  Nucleobase Analogue Donor–Acceptor Pairs**

donor	$\Phi_f$	$n^a$	$J/M^{-1}\text{ cm}^{-1}\text{ nm}^4$	$R_0/\text{\AA}$
Monomer <sup>b</sup>				
$tC$	0.13	1.35	$4.7 \times 10^{13}$	21.8
$tC^O$	0.30	1.35	$1.0 \times 10^{14}$	28.5
In dsDNA <sup>c</sup>				
$tC$	0.20	1.40	$5.4 \times 10^{13}$	23.4
$tC^O$	0.22	1.40	$1.2 \times 10^{14}$	27.2

<sup>a</sup> Since the refractive index is a macroscopic property, the chosen value of 1.40 is an approximate guess based on the chemical structure of the DNA molecule. <sup>b</sup> Quantum yield values are for the nucleosides. <sup>c</sup> Since the quantum yields of  $tC$  and  $tC^O$  are slightly dependent on neighboring bases,<sup>61,62</sup> the values used here are averages.

Furthermore, representative values of the critical Förster distances are shown in Table 1 assuming  $\kappa^2 = 2/3$  (freely rotating chromophores) and averaged donor quantum yields.<sup>80</sup> The overlap integrals between the absorption of monomeric  $tC_{\text{nitro}}$  and the emission of monomeric  $tC$  and  $tC^O$  are  $4.7 \times 10^{13}$  and  $1.0 \times 10^{14}\text{ M}^{-1}\text{ cm}^{-1}\text{ nm}^4$ , respectively. The corresponding critical distances are  $21.8\text{ \AA}$  between monomeric  $tC$ – $tC_{\text{nitro}}$  and  $28.5\text{ \AA}$  between  $tC^O$ – $tC_{\text{nitro}}$ . Due to the red-shifted absorption of  $tC_{\text{nitro}}$  upon incorporation into DNA, the overlap integrals for FRET pairs positioned in DNA are slightly larger compared to the monomeric FRET pairs ( $5.4 \times 10^{13}$  and  $1.2 \times 10^{14}\text{ M}^{-1}\text{ cm}^{-1}\text{ nm}^4$  for  $tC$  and  $tC^O$  as donors, respectively). Using the average quantum yields of  $tC$  and  $tC^O$  positioned in DNA, the corresponding critical distances become  $23.4\text{ \AA}$  for  $tC$  as the donor and  $27.2\text{ \AA}$  for  $tC^O$  as the donor. These values may be compared to the dimensions of the B-DNA double helix which has a length of approximately  $34\text{ \AA}$  per turn.

Since the Förster formulation is based on a point dipole approximation, it is noted here that the FRET theory is not valid for close lying chromophores in which electronic couplings of other origins can be anticipated.<sup>97</sup> We have previously performed circular dichroism experiments on homodimers of  $tC$  as well as  $tC^O$  separated by 0–2 bases in DNA duplexes to examine the excitonic effect and found minor effects for the case where the homodimer is separated only by 0 bases (data not shown). The dipole–dipole resonance mechanism is therefore expected to be the totally predominant electronic interaction between these base analogues in the distance range in which they operate (appr.  $15$ – $45\text{ \AA}$ ).

## Conclusions and Outlook

We have characterized the nucleobase analogue  $tC_{\text{nitro}}$  with special focus put on its use as a FRET acceptor in nucleic acid studies. With a  $pK_a$  of 11.1, the neutral form of  $tC_{\text{nitro}}$  is totally predominant under physiological conditions. The lowest energy absorption band ( $375$ – $525\text{ nm}$ ) of this compound is the result of a single electronic transition well separated ( $\sim 1\text{ eV}$ ) from higher energy excitations and associated with an in-plane polarized transition dipole moment oriented  $\sim 27^\circ$  toward the nitro group from the molecular long axis. A DFT conformational search performed at the B3LYP/6-31G(d,p) level identified two local minima on the potential energy surface of  $tC_{\text{nitro}}$  corresponding to two geometries folded along the middle sulfur–nitrogen axis; however, the direction of the transition dipole moment of  $tC_{\text{nitro}}$  is virtually the same within its two geometries.

Currently available FRET pairs for use in nucleic acid containing systems normally have longer Förster distances ( $>50$

Å at  $\kappa^2 = 2/3$ ) than the system presented here but lack high control of geometry and/or a stable quantum yield for the donor, resulting in inaccuracies in estimating the Förster distance. This work, on the other hand, lays the foundation for future detailed structural studies of nucleic acid containing systems implementing tC<sub>nitro</sub> as a FRET acceptor and tC or tC<sup>O</sup> as the donor. The fact that these nucleobase donor–acceptor pairs can be rigidly positioned close to or inside the actual site of interest when studying nucleic acids opens up a number of new possibilities in the structural investigation of nucleic acids in solution. Since the energy transfer process is highly dependent on both orientation and distance between the nucleobases, very detailed studies of nucleic acid structures and dynamics are in principle possible. Furthermore, through carefully designed experiments, the nucleobase analogue FRET pairs have the potential to thoroughly probe even subtle structural changes occurring in nucleic acids, e.g., resulting from the sequence specific interaction with other (bio)molecules or a change of physical chemical conditions.

**Acknowledgment.** This research is supported by the Swedish Research Council (VR) and the Danish Council for Independent Research | Natural Sciences (FNU).

## References and Notes

- (1) Herdewijn, P. *Antisense Nucleic Acid Drug Dev.* **2000**, *10*, 297.
- (2) Wojciechowski, F.; Hudson, R. H. E. *Curr. Top. Med. Chem.* **2007**, *7*, 667.
- (3) Wagenknecht, H. A. *Ann. N.Y. Acad. Sci.* **2008**, *1130*, 122.
- (4) Okamoto, A.; Tainaka, K.; Ochi, Y.; Kanatani, K.; Saito, I. *Mol. Biosyst.* **2006**, *2*, 122.
- (5) Venkatesan, N.; Seo, Y. J.; Kim, B. H. *Chem. Soc. Rev.* **2008**, *37*, 648.
- (6) Barhate, N.; Cekan, P.; Massey, A. P.; Sigurdsson, S. T. *Angew. Chem., Int. Ed.* **2007**, *46*, 2655.
- (7) Cekan, P.; Smith, A. L.; Barhate, N.; Robinson, B. H.; Sigurdsson, S. T. *Nucleic Acids Res.* **2008**, *36*, 5946.
- (8) Jung, K. H.; Marx, A. *Cell. Mol. Life Sci.* **2005**, *62*, 2080.
- (9) Asseline, U. *Curr. Org. Chem.* **2006**, *10*, 491.
- (10) Hawkins, M. E. In *Topics in Fluorescence Spectroscopy: DNA Technology*; Lakowicz, J. R., Ed.; Kluwer Academic/Plenum Publishers: New York, 2003.
- (11) Okamoto, A.; Saito, Y.; Saito, I. *J. Photochem. Photobiol., C* **2005**, *6*, 108.
- (12) Rist, M. J.; Marino, J. P. *Curr. Org. Chem.* **2002**, *6*, 775.
- (13) Wilson, J. N.; Kool, E. T. *Org. Biomol. Chem.* **2006**, *4*, 4265.
- (14) Freese, E. *J. Mol. Biol.* **1959**, *1*, 87.
- (15) Ward, D. C.; Reich, E.; Stryer, L. *J. Biol. Chem.* **1969**, *244*, 1228.
- (16) Hawkins, M. E. *Cell Biochem. Biophys.* **2001**, *34*, 257.
- (17) Hawkins, M. E. In *Methods in Enzymology - Fluorescence Spectroscopy*; Elsevier Academic Press Inc: San Diego, CA, 2008; Vol. 450, p 201.
- (18) Berry, D. A.; Jung, K. Y.; Wise, D. S.; Sercel, A. D.; Pearson, W. H.; Mackie, H.; Randolph, J. B.; Somers, R. L. *Tetrahedron Lett.* **2004**, *45*, 2457.
- (19) Okamoto, A.; Tainaka, K.; Saito, I. *Tetrahedron Lett.* **2003**, *44*, 6871.
- (20) Okamoto, A.; Tainaka, K.; Saito, I. *J. Am. Chem. Soc.* **2003**, *125*, 4972.
- (21) Okamoto, A.; Tanaka, K.; Fukuta, T.; Saito, I. *J. Am. Chem. Soc.* **2003**, *125*, 9296.
- (22) Krueger, A. T.; Lu, H. G.; Lee, A. H. F.; Kool, E. T. *Acc. Chem. Res.* **2007**, *40*, 141.
- (23) Krueger, A. T.; Kool, E. T. *J. Am. Chem. Soc.* **2008**, *130*, 3989.
- (24) Greco, N. J.; Sinkeldam, R. W.; Tor, Y. *Org. Lett.* **2009**, *11*, 1115.
- (25) Mizuta, M.; Seio, K.; Miyata, K.; Sekine, M. *J. Org. Chem.* **2007**, *72*, 5046.
- (26) Srivatsan, S. G.; Weizman, H.; Tor, Y. *Org. Biomol. Chem.* **2008**, *6*, 1334.
- (27) Butler, R. S.; Cohn, P.; Tenzel, P.; Abboud, K. A.; Castellano, R. K. *J. Am. Chem. Soc.* **2009**, *131*, 623.
- (28) Dyrager, C.; Börjesson, K.; Diner, P.; Elf, A.; Albinsson, B.; Wilhelmsson, L. M.; Grötl, M. *Eur. J. Org. Chem.* **2009**, 1515.
- (29) Mizuta, M.; Seio, K.; Ohkubo, A.; Sekine, M. *J. Phys. Chem. B* **2009**, *113*, 9562.
- (30) Miyata, K.; Mineo, R.; Tamamushi, R.; Mizuta, M.; Ohkubo, A.; Taguchi, H.; Seio, K.; Santa, T.; Sekine, M. *J. Org. Chem.* **2007**, *72*, 102.
- (31) Miyata, K.; Tamamushi, R.; Ohkubo, A.; Taguchi, H.; Seio, K.; Santa, T.; Sekine, M. *Org. Lett.* **2006**, *8*, 1545.
- (32) Greco, N. J.; Tor, Y. *J. Am. Chem. Soc.* **2005**, *127*, 10784.
- (33) Wojciechowski, F.; Hudson, R. H. E. *J. Am. Chem. Soc.* **2008**, *130*, 12574.
- (34) Hariharan, C.; Reha-Krantz, L. *J. Biochemistry* **2005**, *44*, 15674.
- (35) Wojtuszewski, K.; Hawkins, M. E.; Cole, J. L.; Mukerji, I. *Biochemistry* **2001**, *40*, 2588.
- (36) Allan, B. W.; Beechem, J. M.; Lindstrom, W. M.; Reich, N. O. *J. Biol. Chem.* **1998**, *273*, 2368.
- (37) Frey, M. W.; Sowers, L. C.; Millar, D. P.; Benkovic, S. J. *Biochemistry* **1995**, *34*, 9185.
- (38) Srivatsan, S. G.; Greco, N. J.; Tor, Y. *Angew. Chem., Int. Ed.* **2008**, *47*, 6661.
- (39) Raney, K. D.; Sowers, L. C.; Millar, D. P.; Benkovic, S. J. *Proc. Natl. Acad. Sci. U.S.A.* **1994**, *91*, 6644.
- (40) Hochstrasser, R. A.; Carver, T. E.; Sowers, L. C.; Millar, D. P. *Biochemistry* **1994**, *33*, 11971.
- (41) Jia, Y. P.; Kumar, A.; Patel, S. S. *J. Biol. Chem.* **1996**, *271*, 30451.
- (42) Ujvari, A.; Martin, C. T. *Biochemistry* **1996**, *35*, 14574.
- (43) Zhong, X. J.; Patel, S. S.; Werneburg, B. G.; Tsai, M. D. *Biochemistry* **1997**, *36*, 11891.
- (44) Holz, B.; Klimasauskas, S.; Serva, S.; Weinhold, E. *Nucleic Acids Res.* **1998**, *26*, 1076.
- (45) Allan, B. W.; Reich, N. O.; Beechem, J. M. *Biochemistry* **1999**, *38*, 5308.
- (46) Allan, B. W.; Reich, N. O. *Biochemistry* **1996**, *35*, 14757.
- (47) Stivers, J. T.; Pankiewicz, K. W.; Watanabe, K. A. *Biochemistry* **1999**, *38*, 952.
- (48) Liu, C. H.; Martin, C. T. *J. Biol. Chem.* **2002**, *277*, 2725.
- (49) Hariharan, C.; Bloom, L. B.; Helquist, S. A.; Kool, E. T.; Reha-Krantz, L. *J. Biochemistry* **2006**, *45*, 2836.
- (50) Liu, C. H.; Martin, C. T. *J. Mol. Biol.* **2001**, *308*, 465.
- (51) Menger, M.; Eckstein, F.; Porschke, D. *Biochemistry* **2000**, *39*, 4500.
- (52) Guest, C. R.; Hochstrasser, R. A.; Sowers, L. C.; Millar, D. P. *Biochemistry* **1991**, *30*, 3271.
- (53) Xu, D. G.; Evans, K. O.; Nordlund, T. M. *Biochemistry* **1994**, *33*, 9592.
- (54) Ramreddy, T.; Kombrabail, M.; Krishnamoorthy, G.; Rao, B. J. *J. Phys. Chem. B* **2009**, *113*, 6840.
- (55) Jean, J. M.; Hall, K. B. *Biochemistry* **2004**, *43*, 10277.
- (56) Ramreddy, T.; Rao, B. J.; Krishnamoorthy, G. *J. Phys. Chem. B* **2007**, *111*, 5757.
- (57) Larsen, O. F. A.; van Stokkum, I. H. M.; Gobets, B.; van Grondelle, R.; van Amerongen, H. *Biophys. J.* **2001**, *81*, 1115.
- (58) Dash, C.; Rausch, J. W.; Le Grice, S. F. *J. Nucleic Acids Res.* **2004**, *32*, 1539.
- (59) Börjesson, K.; Sandin, P.; Wilhelmsson, L. M. *Biophys. Chem.* **2009**, *139*, 24.
- (60) Engman, K. C.; Sandin, P.; Osborne, S.; Brown, T.; Billeter, M.; Lincoln, P.; Nordén, B.; Albinsson, B.; Wilhelmsson, L. M. *Nucleic Acids Res.* **2004**, *32*, 5087.
- (61) Sandin, P.; Börjesson, K.; Li, H.; Mårtensson, J.; Brown, T.; Wilhelmsson, L. M.; Albinsson, B. *Nucleic Acids Res.* **2008**, *36*, 157.
- (62) Sandin, P.; Wilhelmsson, L. M.; Lincoln, P.; Powers, V. E. C.; Brown, T.; Albinsson, B. *Nucleic Acids Res.* **2005**, *33*, 5019.
- (63) Wilhelmsson, L. M.; Holmén, A.; Lincoln, P.; Nielson, P. E.; Nordén, B. *J. Am. Chem. Soc.* **2001**, *123*, 2434.
- (64) Wilhelmsson, L. M.; Sandin, P.; Holmén, A.; Albinsson, B.; Lincoln, P.; Nordén, B. *J. Phys. Chem. B* **2003**, *107*, 9094.
- (65) Stengel, G.; Gill, J. P.; Sandin, P.; Wilhelmsson, L. M.; Albinsson, B.; Nordén, B.; Millar, D. *Biochemistry* **2007**, *46*, 12289.
- (66) Börjesson, K.; Preus, S.; El-Sagheer, A. H.; Brown, T.; Albinsson, B.; Wilhelmsson, L. M. *J. Am. Chem. Soc.* **2009**, *131*, 4288.
- (67) Clegg, R. M.; Murchie, A. I. H.; Zechel, A.; Lilley, D. M. *J. Proc. Natl. Acad. Sci. U.S.A.* **1993**, *90*, 2994.
- (68) Hurley, D. J.; Tor, Y. *J. Am. Chem. Soc.* **2002**, *124*, 13231.
- (69) Iqbal, A.; Arslan, S.; Okumus, B.; Wilson, T. J.; Giraud, G.; Norman, D. G.; Ha, T.; Lilley, D. M. *J. Proc. Natl. Acad. Sci. U.S.A.* **2008**, *105*, 11176.
- (70) Lewis, F. D.; Zhang, L. G.; Zuo, X. B. *J. Am. Chem. Soc.* **2005**, *127*, 10002.
- (71) Sapsford, K. E.; Berti, L.; Medintz, I. L. *Angew. Chem., Int. Ed.* **2006**, *45*, 4562.
- (72) Eldrup, A. B.; Nielsen, B. B.; Haaima, G.; Rasmussen, H.; Kastrop, J. S.; Christensen, C.; Nielsen, P. E. *Eur. J. Org. Chem.* **2001**, 1781.
- (73) Becke, A. D. *J. Chem. Phys.* **1993**, *98*, 5648.
- (74) Lee, C. T.; Yang, W. T.; Parr, R. G. *Phys. Rev. B* **1988**, *37*, 785.
- (75) Stephens, P. J.; Devlin, F. J.; Chabalowski, C. F.; Frisch, M. J. *J. Phys. Chem.* **1994**, *98*, 11623.
- (76) Frisch, M. J.; Trucks, G. W.; Schlegel, H. B.; Scuseria, G. E.; Robb, M. A.; Cheeseman, J. R.; Montgomery, J. A., Jr.; Vreven, T.; Kudin, K. N.



- Burant, J. C.; Millam, J. M.; Iyengar, S. S.; Tomasi, J.; Barone, V.; Mennucci, B.; Cossi, M.; Scalmani, G.; Rega, N.; Petersson, G. A.; Nakatsuji, H.; Hada, M.; Ehara, M.; Toyota, K.; Fukuda, R.; Hasegawa, J.; Ishida, M.; Nakajima, T.; Honda, Y.; Kitao, O.; Nakai, H.; Klene, M.; Li, X.; Knox, J. E.; Hratchian, H. P.; Cross, J. B.; Bakken, V.; Adamo, C.; Jaramillo, J.; Gomperts, R.; Stratmann, R. E.; Yazyev, O.; Austin, A. J.; Cammi, R.; Pomelli, C.; Ochterski, J. W.; Ayala, P. Y.; Morokuma, K.; Voth, G. A.; Salvador, P.; Dannenberg, J. J.; Zakrzewski, V. G.; Dapprich, S.; Daniels, A. D.; Strain, M. C.; Farkas, O.; Malick, D. K.; Rabuck, A. D.; Raghavachari, K.; Foresman, J. B.; Ortiz, J. V.; Cui, Q.; Baboul, A. G.; Clifford, S.; Cioslowski, J.; Stefanov, B. B.; Liu, G.; Liashenko, A.; Piskorz, P.; Komaromi, I.; Martin, R. L.; Fox, D. J.; Keith, T.; Al-Laham, M. A.; Peng, C. Y.; Nanayakkara, A.; Challacombe, M.; Gill, P. M. W.; Johnson, B.; Chen, W.; Wong, M. W.; Gonzalez, C.; Pople, J. A. *Gaussian 03*; Gaussian, Inc.: Wallingford, CT, 2004.
- (77) Marques, M. A. L.; Gross, E. K. U. *Annu. Rev. Phys. Chem.* **2004**, *55*, 427.
- (78) Burke, K.; Werschnik, J.; Gross, E. K. U. *J. Chem. Phys.* **2005**, *123*.
- (79) Rodger, A.; Nordén, B. *Circular Dichroism and Linear Dichroism*; Oxford University Press: Oxford, UK, 1997.
- (80) Lakowicz, J. R. *Principles of Fluorescence Spectroscopy*, 3rd ed.; Springer: New York, 2006; Vol. 3.
- (81) Mason, W. M. *Magnetic Circular Dichroism*; John Wiley & Sons: Hoboken, NJ, 2007.
- (82) Hendler, R. W.; Shrager, R. I. *J. Biochem. Biophys. Methods* **1994**, *28*, 1.
- (83) Bell, J. D.; Blount, J. F.; Briscoe, O. V.; Freeman, H. C. *Chem. Commun.* **1968**, 1656.
- (84) McDowell, J. J. H. *Acta Crystallogr., Sect. B* **1976**, *32*, 5.
- (85) Mohammed, O. F.; Vauthey, E. *J. Phys. Chem. A* **2008**, *112*, 3823.
- (86) Khalil, O. S.; Bach, H. G.; McGlynn, S. P. *J. Mol. Spectrosc.* **1970**, *35*, 455.
- (87) Mikula, J. J.; Stuebing, E. W.; Anderson, R. W.; Harris, L. E. *J. Mol. Spectrosc.* **1972**, *42*, 350.
- (88) Zugazagoitia, J. S.; Almora-Diaz, C. X.; Peon, J. *J. Phys. Chem. A* **2008**, *112*, 358.
- (89) Dreuw, A.; Head-Gordon, M. *J. Am. Chem. Soc.* **2004**, *126*, 4007.
- (90) Dreuw, A.; Weisman, J. L.; Head-Gordon, M. *J. Chem. Phys.* **2003**, *119*, 2943.
- (91) Tozer, D. J. *J. Chem. Phys.* **2003**, *119*, 12697.
- (92) Nordén, B. *J. Chem. Phys.* **1980**, *72*, 5032.
- (93) Ohtani, H.; Kobayashi, T.; Suzuki, K.; Nagakura, S. *Bull. Chem. Soc. Jpn.* **1980**, *53*, 43.
- (94) Morales-Cueto, R.; Esquivelzeta-Rabell, M.; Saucedo-Zugazagoitia, J.; Peon, J. *J. Phys. Chem. A* **2007**, *111*, 552.
- (95) Takezaki, M.; Hirota, N.; Terazima, M. *J. Phys. Chem. A* **1997**, *101*, 3443.
- (96) Kovalenko, S. A.; Schanz, R.; Farztdinov, V. M.; Hennig, H.; Ernsting, N. P. *Chem. Phys. Lett.* **2000**, *323*, 312.
- (97) Beljonne, D.; Curutchet, C.; Scholes, G. D.; Silbey, R. J. *J. Phys. Chem. B* **2009**, *113*, 6583.

JP909471B